Quarkonium in cold nuclear matter and nuclear parton densities

R. Vogt

Physics Division, Lawrence Livermore National Laboratory, Livermore, CA 94551, USA

Physics Department, University of California, Davis, CA 95616, USA

J/ψ Production in $\sqrt{s_{NN}} = 5$ TeV p+Pb Collisions

- **Assumptions of production calculation**
- **Comparison of pp and p+Pb p_T and rapidity distributions with proton PDF**
- **Calculations of $R_{p\mathrm{Pb}}(p_T)$ at forward, backward and midrapidity, $R_{p\mathrm{Pb}}(y)$, and forward/backward ratios $R_{FB}(p_T)$ and $R_{FB}(y)$**
  - **EPS09 with uncertainties, LO vs NLO**
  - **Central EPS09 compared to nDS, nDSg and EKS98**
  - **Mass and scale uncertainties of ratio**
- **Factorization of cold matter effects: R_{PbPb} vs $R_{p\mathrm{Pb}} \times R_{\mathrm{Pb}p}$**

Cold Nuclear Matter Effects in Hadroproduction

In heavy-ion collisions, one has to fold in cold matter effects, typically studied in pA or dA interactions from fixed-target energies to colliders

Hard probes, where production is calculable in QCD, are best to study differences between initial and final state effects

Important cold nuclear matter effects in hadroproduction include:

- **Initial-state nuclear effects on the parton densities (nPDFs)**
- **Initial- (or final-) state energy loss**
- **Final-state absorption on nucleons**
- **Final-state break up by comovers (hadrons or partons)**
- **Intrinsic $Q\overline{Q}$ pairs**

In this talk, I will concentrate on nuclear parton densities, not including any other effect

NLO CEM + EPS09 NLO nPDFs Based on Fitting $\sigma_{c\overline{c}}$

Caveat: full NNLO cross section unknown, could still be large corrections

Employ $m = 1.27$ GeV, lattice value at $m(3\,\mathrm{GeV})$ and use subset of $c\overline{c}$ total cross section data to fix μ_F/m $(2.1^{+2.55}_{-0.85})$ and μ_R/m $(1.6^{+0.11}_{-0.12})$ with CT10 PDFs

Result with $\Delta\chi^2 = 1$ gives uncertainty on scale parameters; $\Delta\chi^2 = 2.3$ gives one standard deviation on total cross section, expect results on $b\overline{b}$ and Υ soon

LHC $pp \to c\overline{c}$ at $\sqrt{s} = 7$ TeV not included but agrees well

The $c\overline{c}$ mass and scale parameters are used to calculate J/ψ

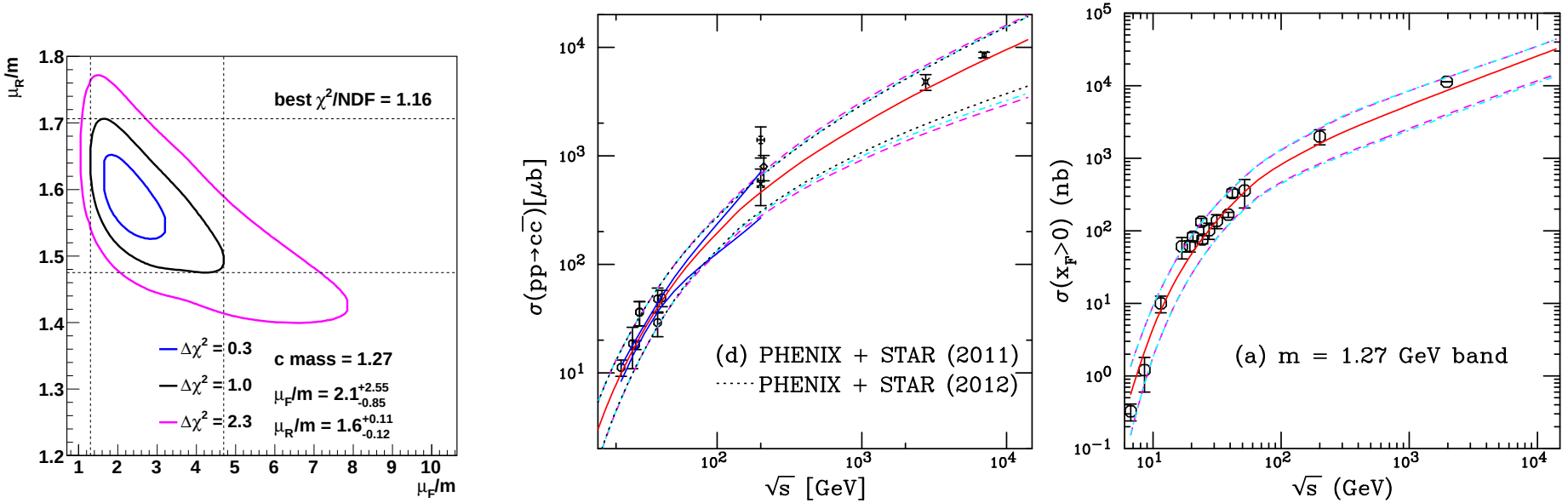

Figure 1: (Left) The χ^2/dof contours for fits including the STAR 2011 cross section but excluding the STAR 2004 cross section. The best fit values are given for the furthest extent of the $\Delta\chi^2 = 1$ contours. (Center) The energy dependence of the charm total cross section compared to data. The best fit values are given for the furthest extent of the $\Delta\chi^2 = 1$ contours. The central value of the fit in each case is given by the solid red curve while the dashed magenta curves and dot-dashed cyan curves show the extent of the corresponding uncertainty bands. The dashed curves outline the most extreme limits of the band. In addition, the dotted black curves show the uncertainty bands obtained with the 2012 STAR results while the solid blue curves in the range $19.4 \le \sqrt{s} \le 200$ GeV represent the uncertainty obtained from the extent of the $\Delta\chi^2 = 2.3$ contour. (Right) The uncertainty band on the forward J/ψ cross section. The dashed magenta curves and dot-dashed cyan curves show the extent of the corresponding uncertainty bands. The dashed curves outline the most extreme limits of the band. (RV, R Nelson and A D Frawley)

Comparing $pp \to J/\psi$ Production by Different Proton PDFs I: Distributions

Here we compare the *shapes* of the p_T and rapidity distributions from CT10 with CTEQ5M, CTEQ6M and MSTW, all calculated with the same mass and scale parameters at $\sqrt{s} = 5$ TeV

Cross sections normalized to CT10 value

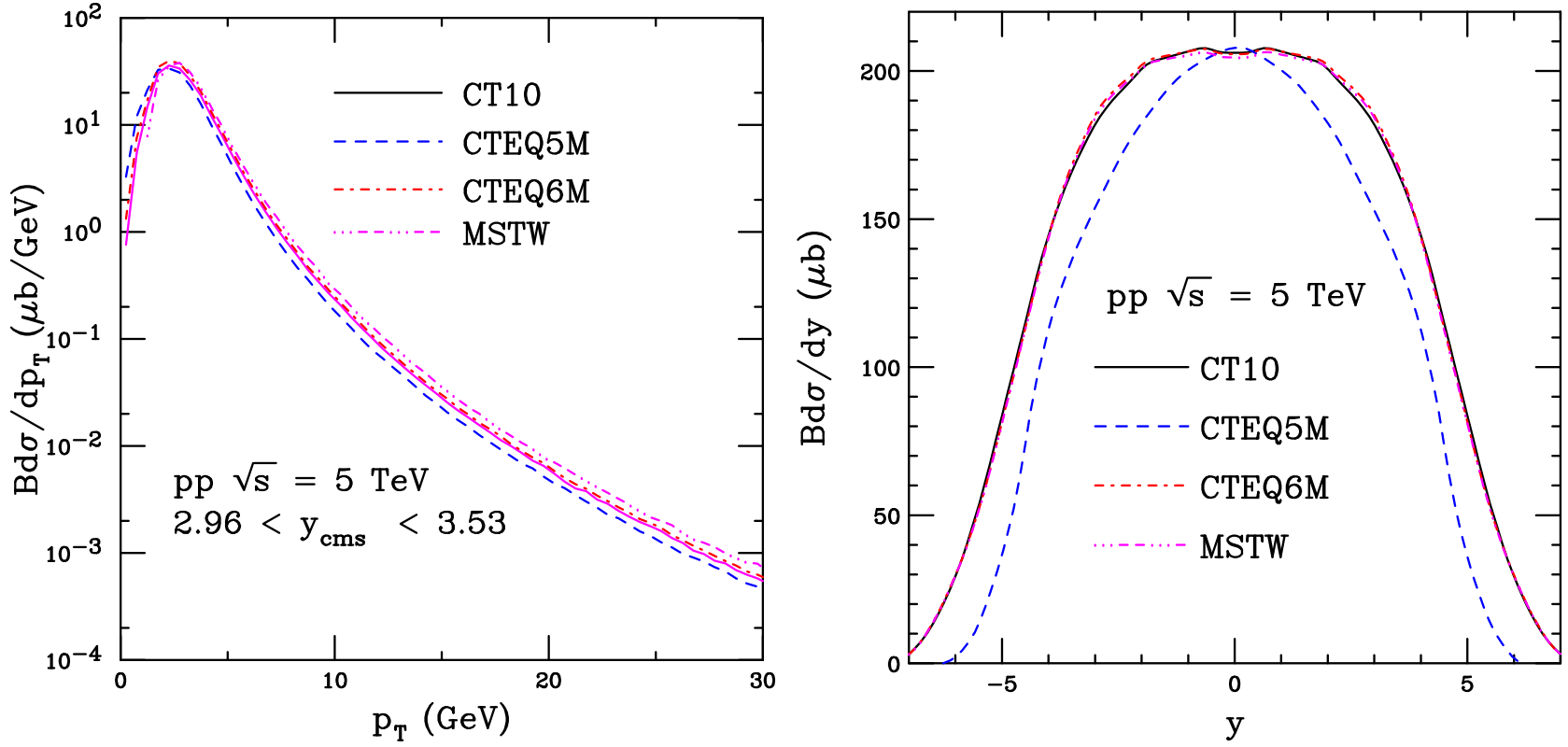

Figure 2: **The J/ψ p_T distribution at forward rapidity in pp collisions (left) and the p_T-integrated y distribution (right). Shapes from CT10 (black), CTEQ5M (blue), CTEQ6M (red) and MSTW (magenta) are compared, all calculated with the same input parameters.**

Comparing $pp \to J/\psi$ Production by Different Proton PDFs II: Ratios

To better compare the *shapes* of the p_T and rapidity distributions relative to CT10, we take the ratios of other PDFs to CT10 with both cross sections normalized to CT10 value: similar slope for $p_T > 5$ GeV, CTEQ5M y distribution considerably narrower

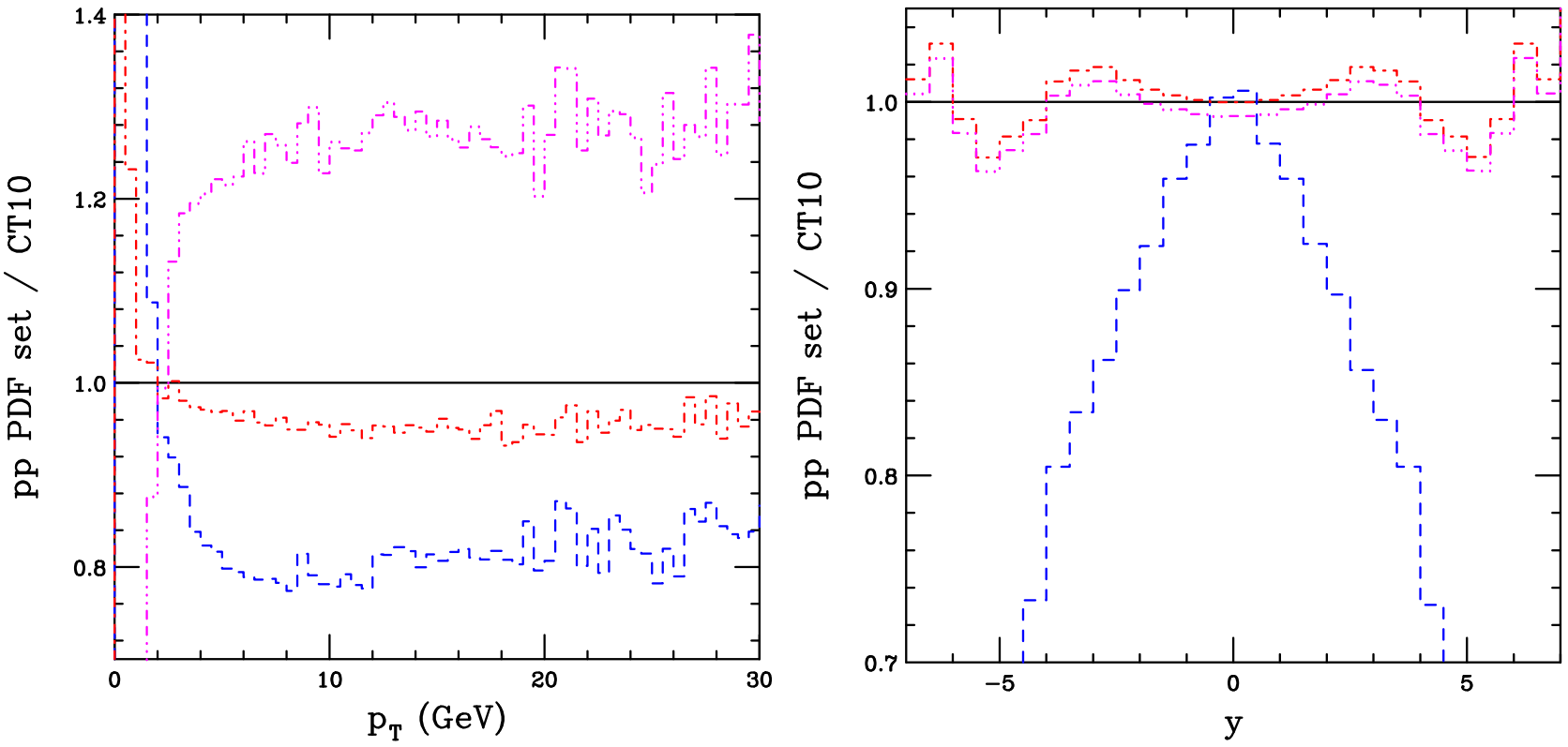

Figure 3: **The ratios of the J/ψ p_T distribution at forward rapidity in pp collisions (left) and the p_T-integrated y distribution (right) with CTEQ5M (blue), CTEQ6M (red) and MSTW (magenta) relative to CT10.**

Nuclear PDFs at NLO

Gluon shadowing ratios compared at the J/ψ and Υ production scales

EPS09 NLO (black) and EKS98 LO (magenta) very similar for $x > 0.002$, significant antishadowing, nDS NLO (blue) and nDSg NLO (red) have almost no antishadowing, nDSg and EKS98 have stronger shadowing than central EPS09 at low x

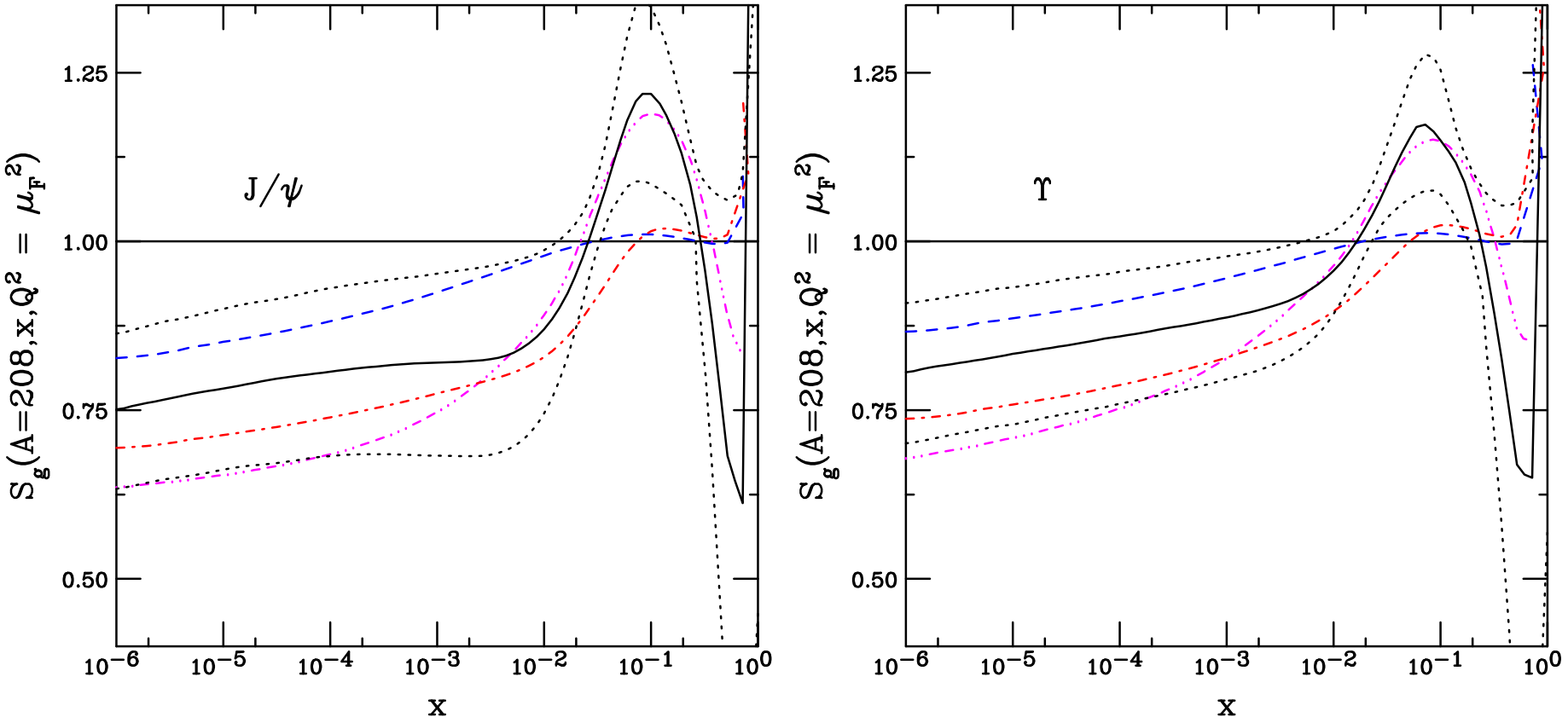

Figure 4: **Gluon shadowing ratios calculated for Pb nuclei ($A = 208$) calculated at the central value of the fitted factorization scales for J/psi (left) and Υ (right). EPS09 NLO is shown by the black solid curve while the uncertainty band is outlined by the black dotted curves. The NLO nDS and nDSg parameterizations are given in the blue dashed and red dot dashed curves. The LO EKS98 parameterization is in magenta (dot-dot-dot-dash-dashed).**

EPS09 Central Ratio Independent of Proton PDF

Even though global fit for EPS09 is based on a specific proton PDF set, the calculated shadowing ratios are basically unchanged by the choice of proton PDF

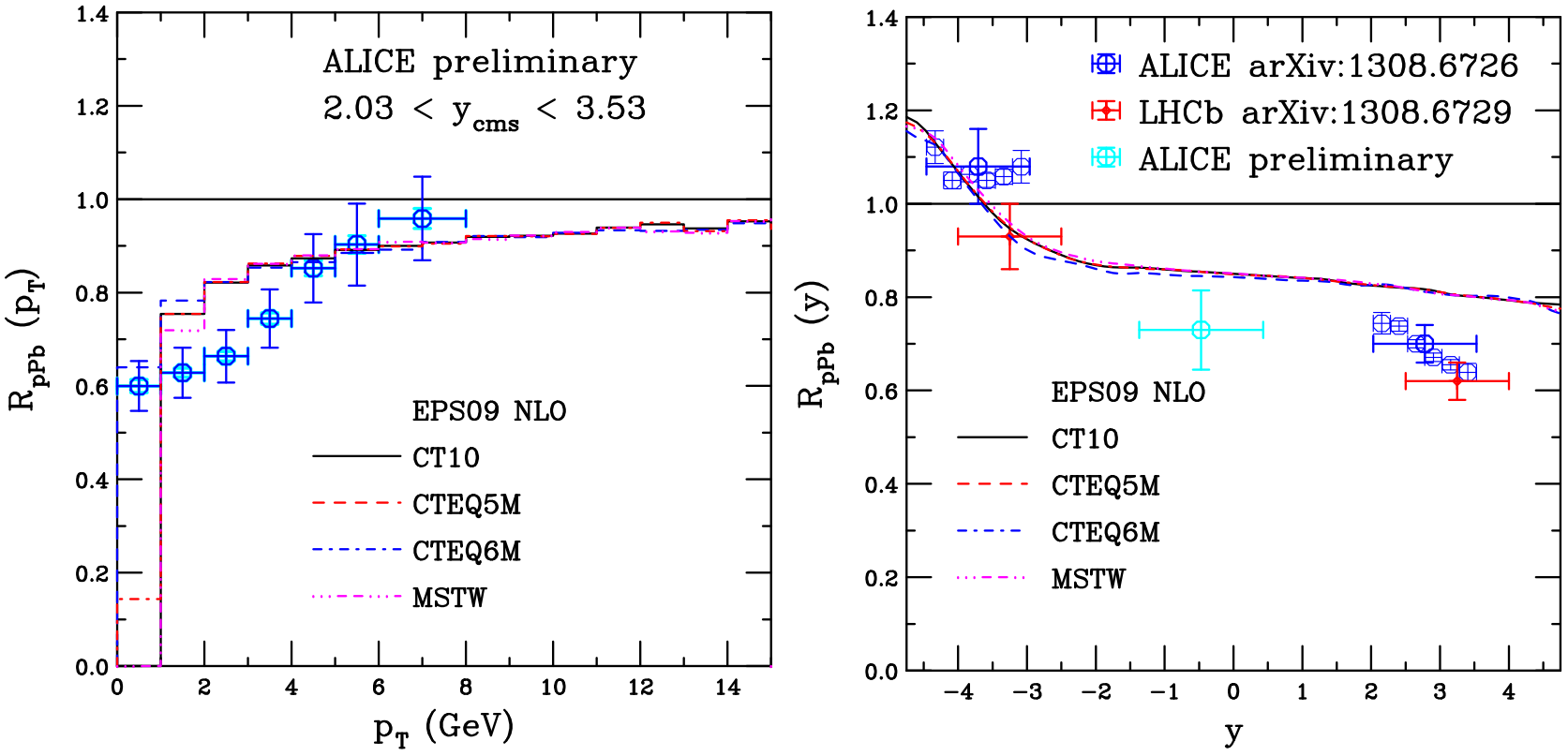

Figure 5: **The ratio $R_{p\mathrm{Pb}}(p_T)$ for ALICE at forward rapidity (left) and p_T-integrated as a function of rapidity. The ratios are for CT10 (black), nDS (blue), nDSg (red) and EKS98 (magenta).**

Calculating nPDF Uncertainties in pA

EPS09 LO and EPS09 NLO based on CTEQ61L and CTEQ6M respectively

The gluon densities in these two sets differ significantly at low x, hence the low x modifications of EPS09 LO and NLO are quite different

nPDF uncertainties calculated with the 30+1 sets of EPS09: one central set and 30 sets obtained by varying each of the 15 parameters, i.e. sets 2 and 3 were obtained by changing parameter 1 by $\pm 1\sigma_1$ *etc.* where σ_i is the standard deviation of parameter i

Uncertainties due to shadowing calculated using 30+1 error sets of EPS09 NLO added in quadrature so the uncertainty is cumulative

EPS09 Uncertainty Bands I: $R_{p\mathrm{Pb}}(p_T)$

Data typically show stronger effect than central EPS09 result alone but the data tend to fall within the uncertainty band

These calculations (also for the rapidity dependence, next slide) differ somewhat from previous results shown – the wrong scale was being passed to the nPDFs

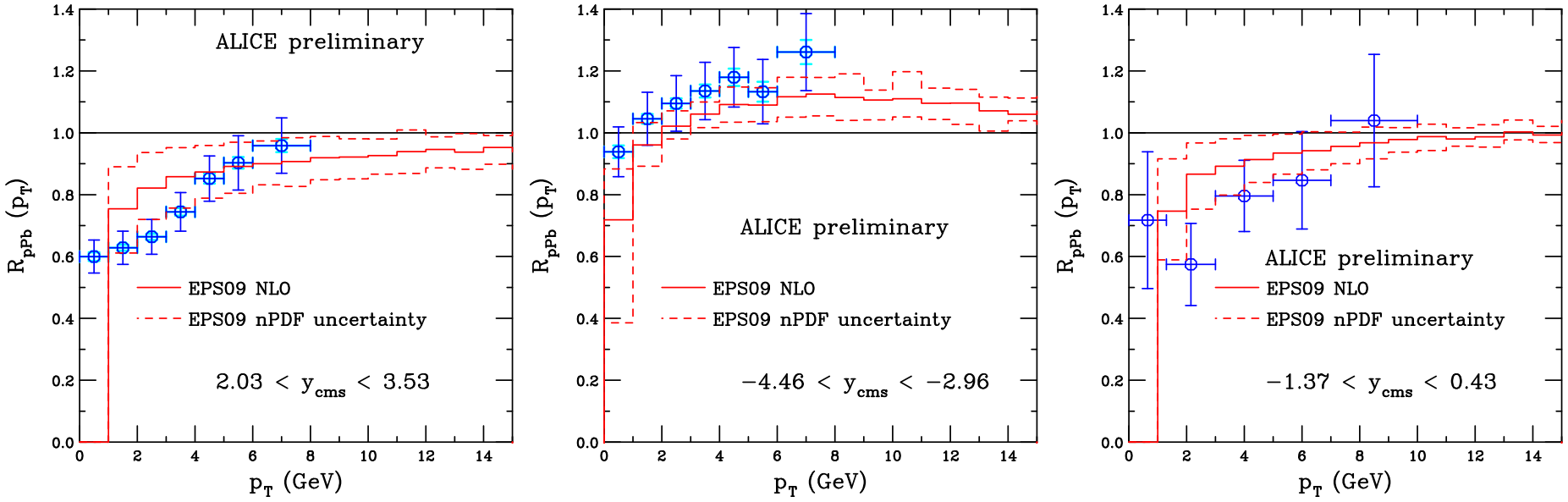

Figure 6: **The ratio $R_{p\mathrm{Pb}}(p_T)$ for ALICE at forward rapidity (left) and backward (middle) and central (right) rapidity. The EPS09 uncertainty band is shown.**

EPS09 Uncertainty Bands II: $R_{p\mathrm{Pb}}(y)$

Backward rapidity data agree with the rise at $y < -2.5$ from antishadowing onset

Preliminary midrapidity point is on the lower edge of the uncertainty band

Forward rapidity data are underestimated, only the lower edge of the uncertainty band (strongest shadowing) is consistent with data

For $y > -2.5$, the band is relatively wide, about $\pm 12\%$, and $R_{p\mathrm{Pb}}$ decreases by less than 10% in this region

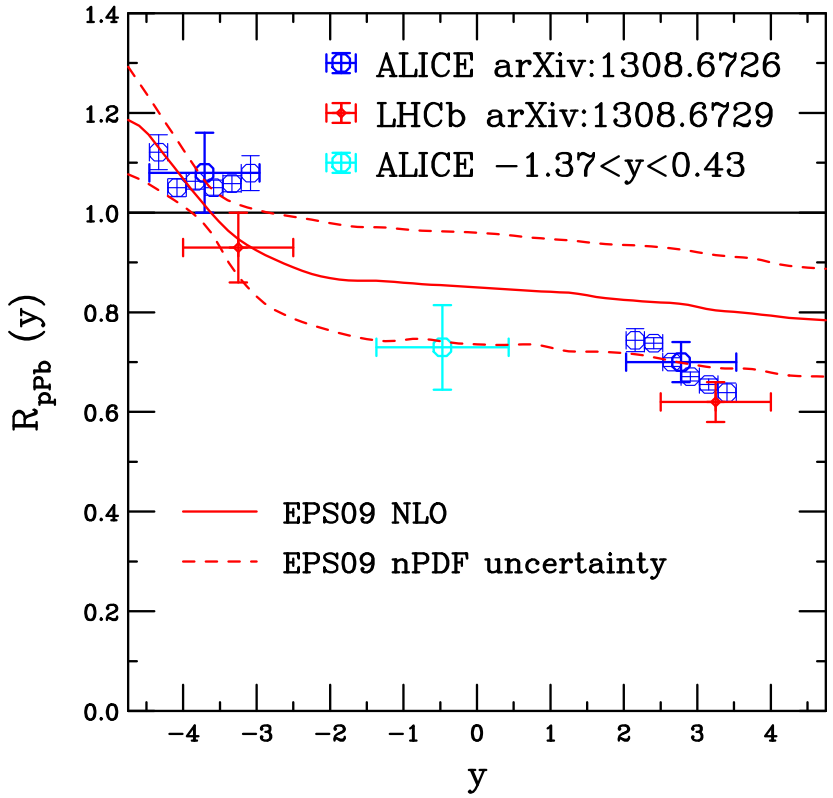

Figure 7: **The EPS09 NLO uncertainty band, $R_{p\mathrm{Pb}}(y)$.**

EPS09 Uncertainty Bands III: R_{FB}

Reduced uncertainties in the forward/backward ratio because we take the ratio before adding differences in quadrature

The p_T ratio almost flat and above the data for $p_T < 6$ GeV

Curvature of rapidity ratio at $y > 2.5$ reflects the antishadowing rise at backward rapidity and the narrower uncertainty band in this region relative to the forward region

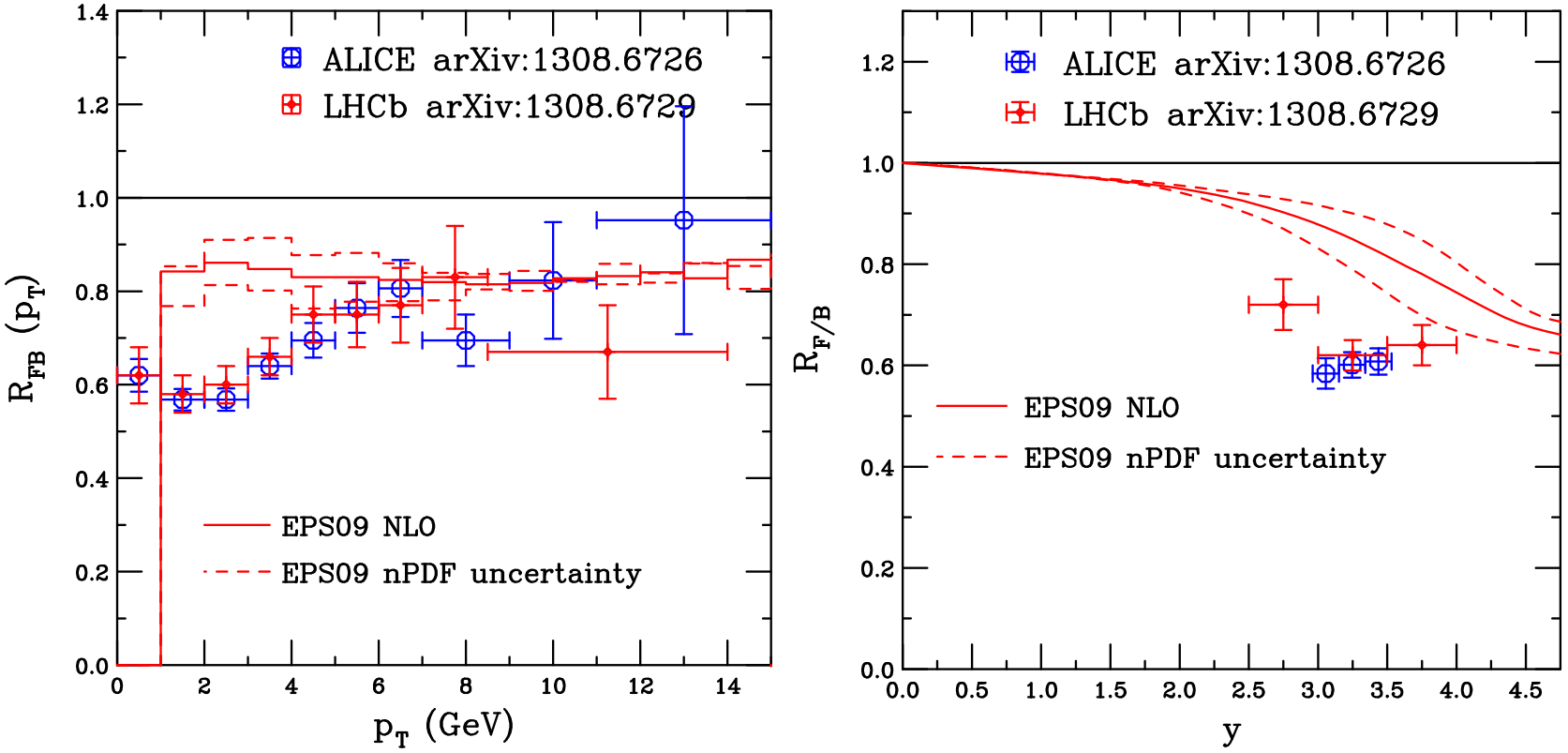

Figure 8: **The ratio $R_{p\mathrm{Pb}}(p_T)$ for ALICE at forward rapidity (left) and p_T-integrated as a function of rapidity (right). The EPS09 uncertainty band is shown.**

NLO vs LO EPS09

The nPDF set used should be appropriate to the order of the calculation: if the LO set in a NLO calculation agrees better with the data, it's not generally better

A NLO calculation is required for J/ψ in CEM to obtain p_T distribution

LO CEM uncertainty band is broader, with stronger shadowing, to counterbalance the flatter low x behavior of CTEQ61L: disparate starting proton PDFs makes it difficult to get good order-by-order agreement of $R_{p\mathrm{Pb}}$

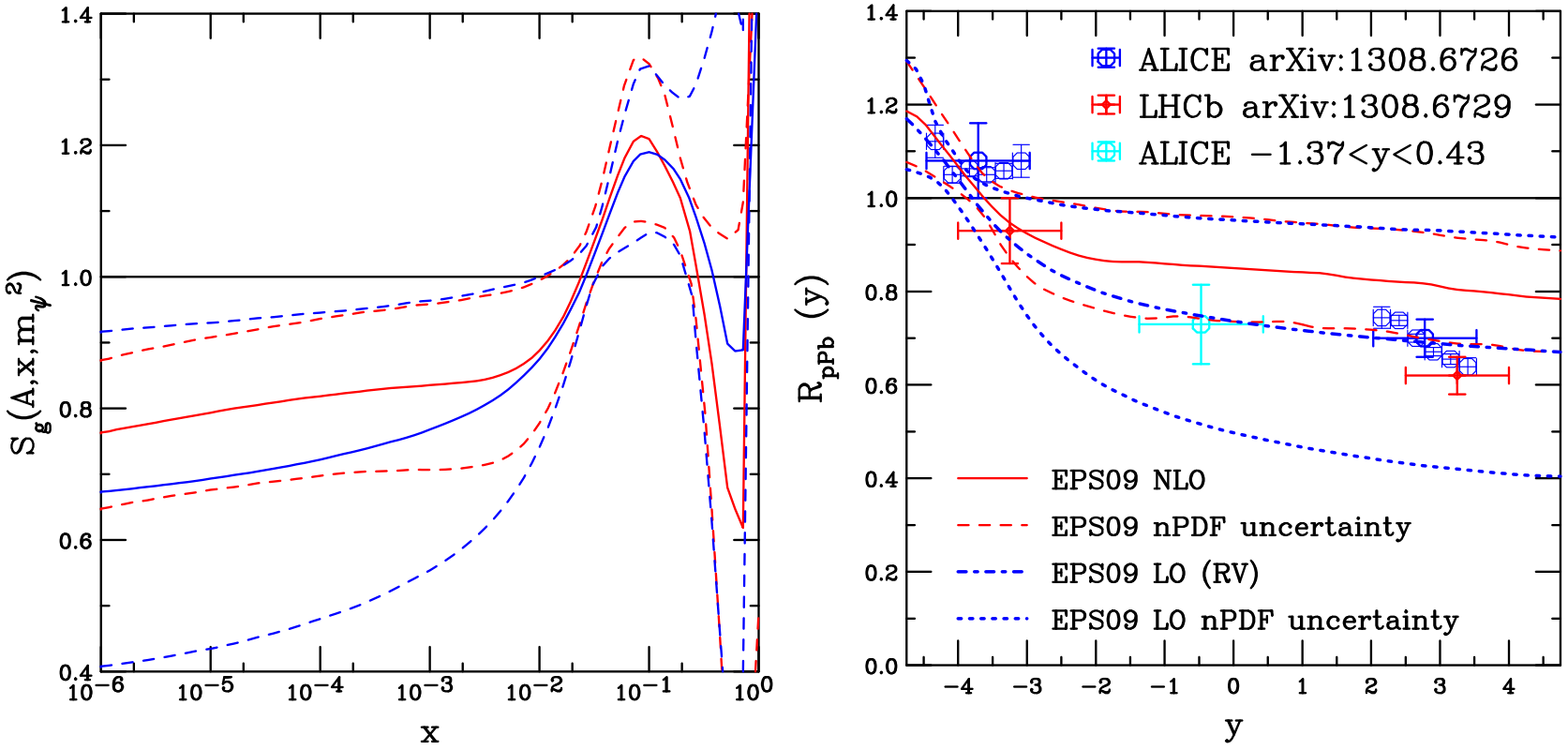

Figure 9: **(Left) The EPS09 LO (blue) and NLO (red) uncertainty bands for gluon shadowing. (Right) The corresponding uncertainty bands for $R_{p\mathrm{Pb}}(y)$ at $\sqrt{s_{NN}} = 5$ TeV.**

EPS09 vs Other nPDFs I: $R_{p\mathrm{Pb}}(p_T)$

Central EPS09 NLO set compared to nDS NLO, nDSg NLO and EKS98 (LO)

nDS effect is weakest of all while nDSg is weak at backward rapidity but stronger than EPS09 at mid- and forward rapidity

EKS98 and EPS09 NLO are very similar for $x > 0.01$ so they agree well at backward and mid-rapidity while EKS98 is stronger at forward rapidity

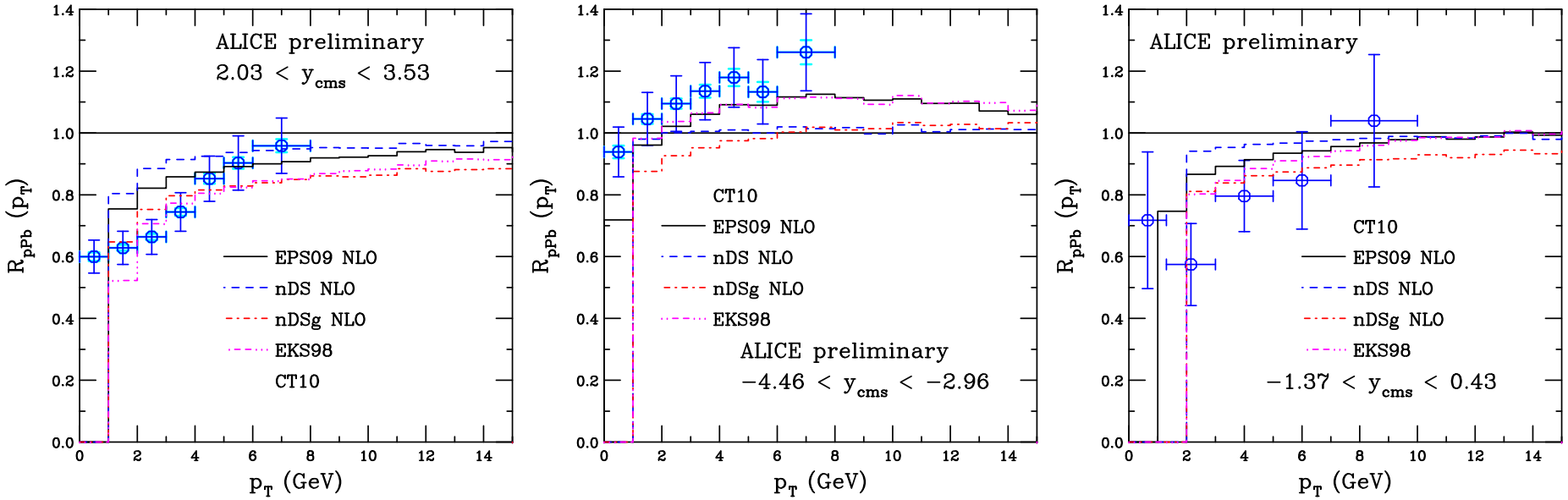

Figure 10: **The ratio $R_{p\mathrm{Pb}}(p_T)$ for ALICE at forward (left), backward (center) and mid- (right) rapidity. The ratios are for central EPS09 NLO (black), nDS NLO (blue), nDSg NLO (red) and EKS98 LO (magenta).**

EPS09 vs Other nPDFs II: $R_{p\mathrm{Pb}}(y)$

EKS98 LO follows EPS09 NLO central set until $y > -2$ where it decreases linearly while EPS09 becomes flatter

EPS09 abrupt change of slope near antishadowing region follows from the gluon shadowing ratio, almost like the low x behavior had to join to assumed antishadowing shape at intermediate x

nDS and nDSg, with no antishadowing, have a weaker y dependence overall

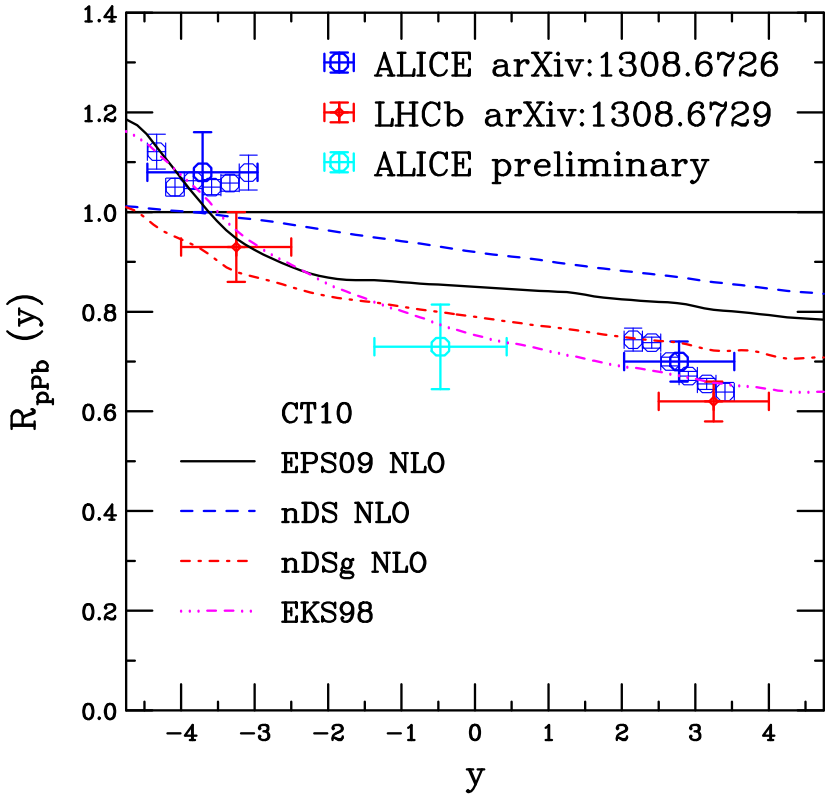

Figure 11: **The calculated $R_{p\mathrm{Pb}}(y)$ for central EPS09 NLO (black), nDS NLO (blue), nDSg NLO (red) and EKS98 LO (magenta).**

EPS09 vs Other nPDFs III: R_{FB}

nDS has strongest p_T dependence of $R_{FB}(p_T)$, EKS98 comes closest to agreement with low p_T data due to the stronger effect at low x than EPS09

Only EPS09 shows curvature in $R_{FB}(y)$, the others show an almost linear y dependence

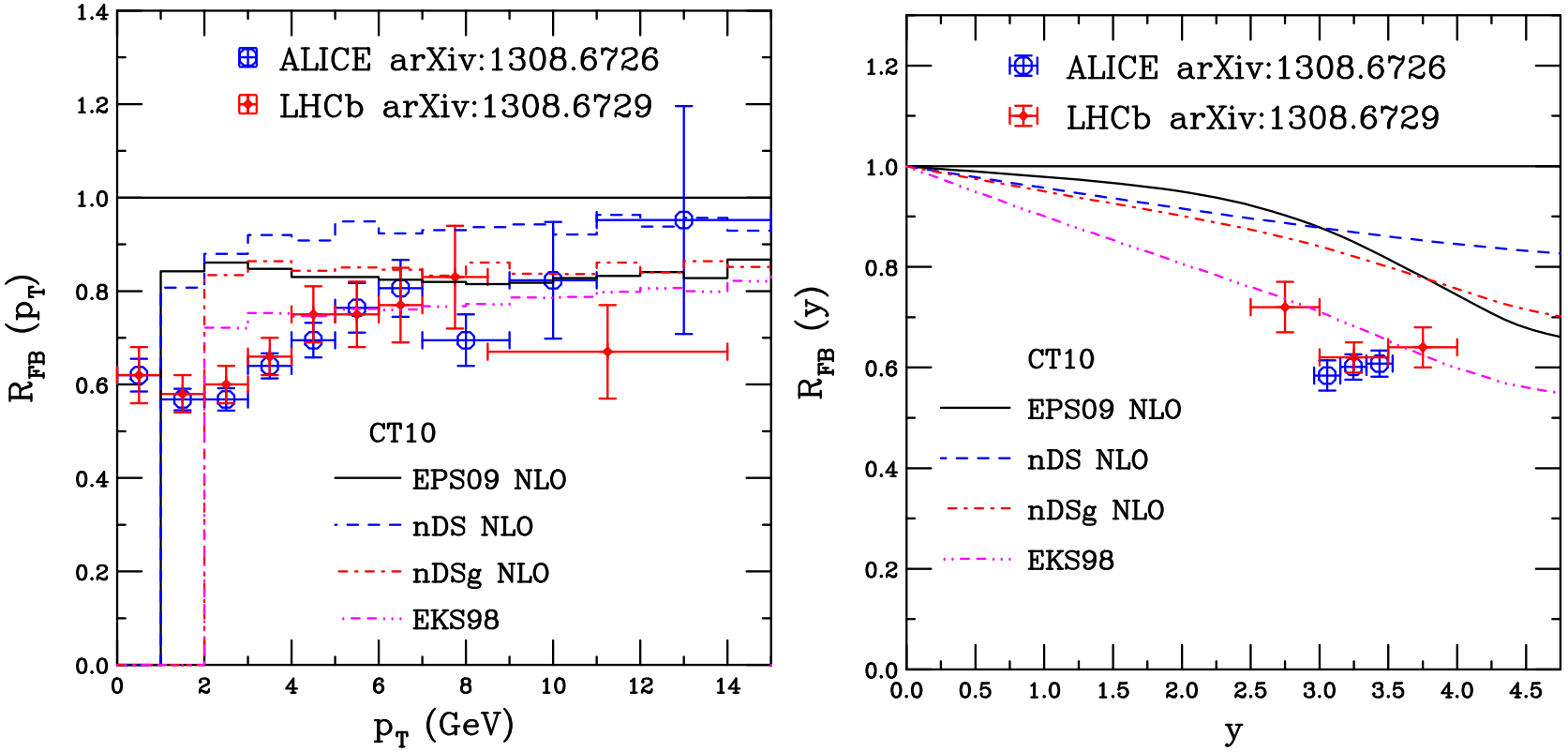

Figure 12: **The ratio $R_{p\mathrm{Pb}}(p_T)$ for ALICE at forward rapidity (left) and p_T-integrated as a function of rapidity. The ratios are for central EPS09 NLO (black), nDS NLO (blue), nDSg NLO (red) and EKS98 LO (magenta).**

Calculating Mass/Scale Uncertainties in Ratios

The one standard deviation uncertainties on the quark mass and scale parameters in the $c\overline{c}$ and J/ψ pp fits were calculated using the CT10 parton densities

EPS09 LO and EPS09 NLO based on CTEQ61L and CTEQ6M respectively

If the central, upper and lower limits of $\mu_{R,F}/m$ are denoted as C, H, and L respectively, then the seven sets corresponding to the scale uncertainty are

$$(\mu_F/m, \mu_R/m) = (C,C), (H,H), (L,L), (C,L), (L,C), (C,H), (H,C)$$

The upper and lower limits of the charm quark mass are used with the central values of μ_F/m and μ_R/m

Three Methods Checked

We calculate the mass and scale uncertainties in 3 ways:

The first two follow Cacciari, Nason and RV where the cross section extremes with mass and scale are used to calculate the uncertainty

$$\sigma_{\rm max} = \sigma_{\rm cent} + \sqrt{(\sigma_{\mu,\rm max} - \sigma_{\rm cent})^2 + (\sigma_{m,\rm max} - \sigma_{\rm cent})^2} \ ,$$
$$\sigma_{\rm min} = \sigma_{\rm cent} - \sqrt{(\sigma_{\mu,\rm min} - \sigma_{\rm cent})^2 + (\sigma_{m,\rm min} - \sigma_{\rm cent})^2} \ ,$$

$m/\mu_F/\mu_R$ **v1 We initially take the ratios of p+Pb to pp for each mass and scale combination and then locate the extrema in each case – this gives the uncertainty on $R_{p\rm Pb}$ of each set, can appear odd if ratios are not very different but the extrema changes between sets**

$m/\mu_F/\mu_R$ **v2 We locate the mass and scale extrema and calculate the uncertainty as above and then form $R_{p\rm Pb}$ by dividing by the pp cross section calculated with the central parameter set – this forms global $R_{p\rm Pb}$ based on the cross sections rather than the shadowing ratios and is thus significantly larger, especially at low p_T, becoming smaller at high p_T (Does not apply to R_{FB})**

$m/\mu_F/\mu_R$ **v3 We add the mass and scale uncertainties in quadrature, a la EPS09, and then form $R_{p\rm Pb}$ by dividing by the central pp cross section – since this is a cumulative uncertainty rather than based on the greatest excursion from the mean, it is the largest uncertainty at low p_T. This was calculated assuming that the appropriate μ_F/m and μ_R/m pairs are $[(H,H),(L,L)]$, $[(H,C),(L,C)]$ and $[(C,H),(C,L)]$, other choices could lead to different results**

Mass and Scale Uncertainty Bands I: $R_{p\mathrm{Pb}}(p_T)$

Uncertainties based on the differences due to EPS09 NLO alone, *i.e.* taking the extrema based on the ratios, gives very small uncertainty, smaller than EPS09 NLO

Uncertainties based on cross sections are much larger with v3 bigger than v2 at low p_T, expected since ratio is cumulative

Ratios decrease at high p_T where the scale choices are less important since $p_T \gg m$

The order switches for the lower limit at high p_T, possibly because of our pairing choices

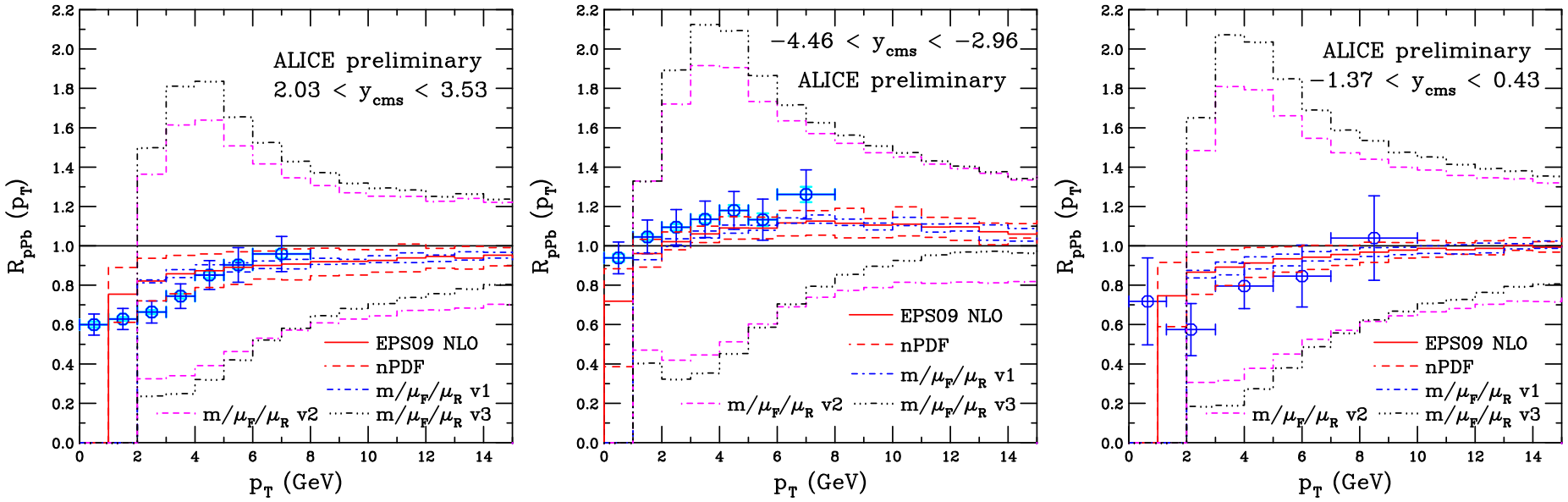

Figure 13: **The mass and scale uncertainties in the ratio $R_{p\mathrm{Pb}}(p_T)$ are compared to those for EPS09 NLO alone for ALICE at forward (left), backward (middle) and mid- (right) rapidity. The EPS09 uncertainty band is shown in red while the uncertainties calculated with method v1 in blue, v2 in magenta and v3 in black.**

EPS09 Uncertainty Bands II: $R_{p\mathrm{Pb}}(y)$

Rapidity dependence with v1 exhibits the perils(?) of basing extrema on individual $R_{p\mathrm{Pb}}$ ratios – when one ratio is larger at high $|y|$ but not at midrapidity, the calculated v1 changes slope at the switching point

Right-hand plot indicates how this happens, the ratio with (H,H) is larger than that of the next highest ratio, that with (C,L) except for $|y|<2$

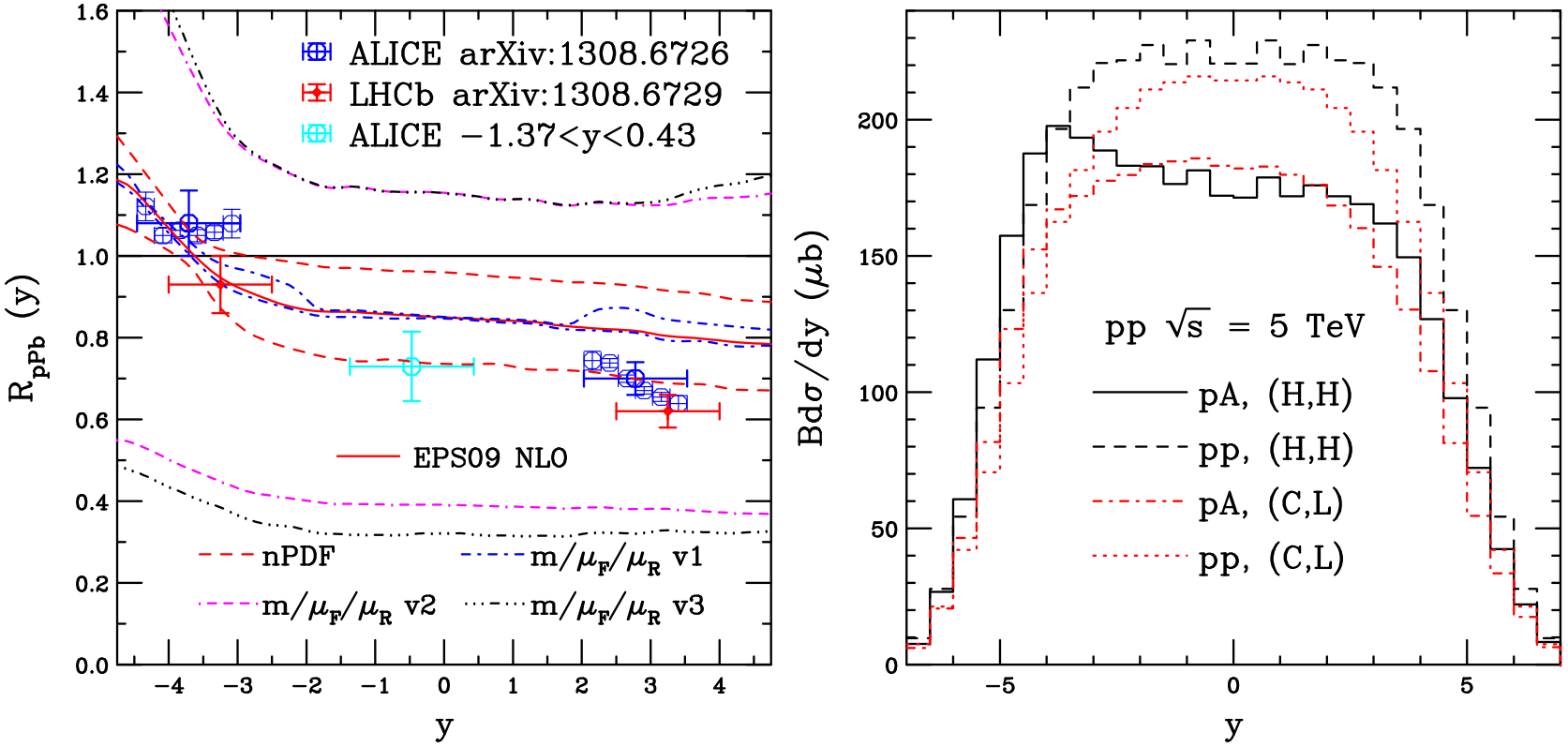

Figure 14: **(Left) The mass and scale uncertainties in the ratio $R_{p\mathrm{Pb}}(y)$ are compared to those for EPS09 NLO alone. The EPS09 uncertainty band is shown in red while the uncertainties calculated with method v1 in blue, v2 in magenta and v3 in black. (Right) The pp and p+Pb rapidity distributions for the (H,H) (C,L) sets showing the differences leading to the change in the upper limit of the mass and scale uncertainties of method v1 around midrapidity.**

EPS09 Uncertainty Bands III: R_{FB}

Only v1 and v3 apply here (v2 is equivalent to v1 in this case)

Taking the forward to backward ratio before calculating the uncertainty band makes this ratio essentially insensitive to the mass and scale

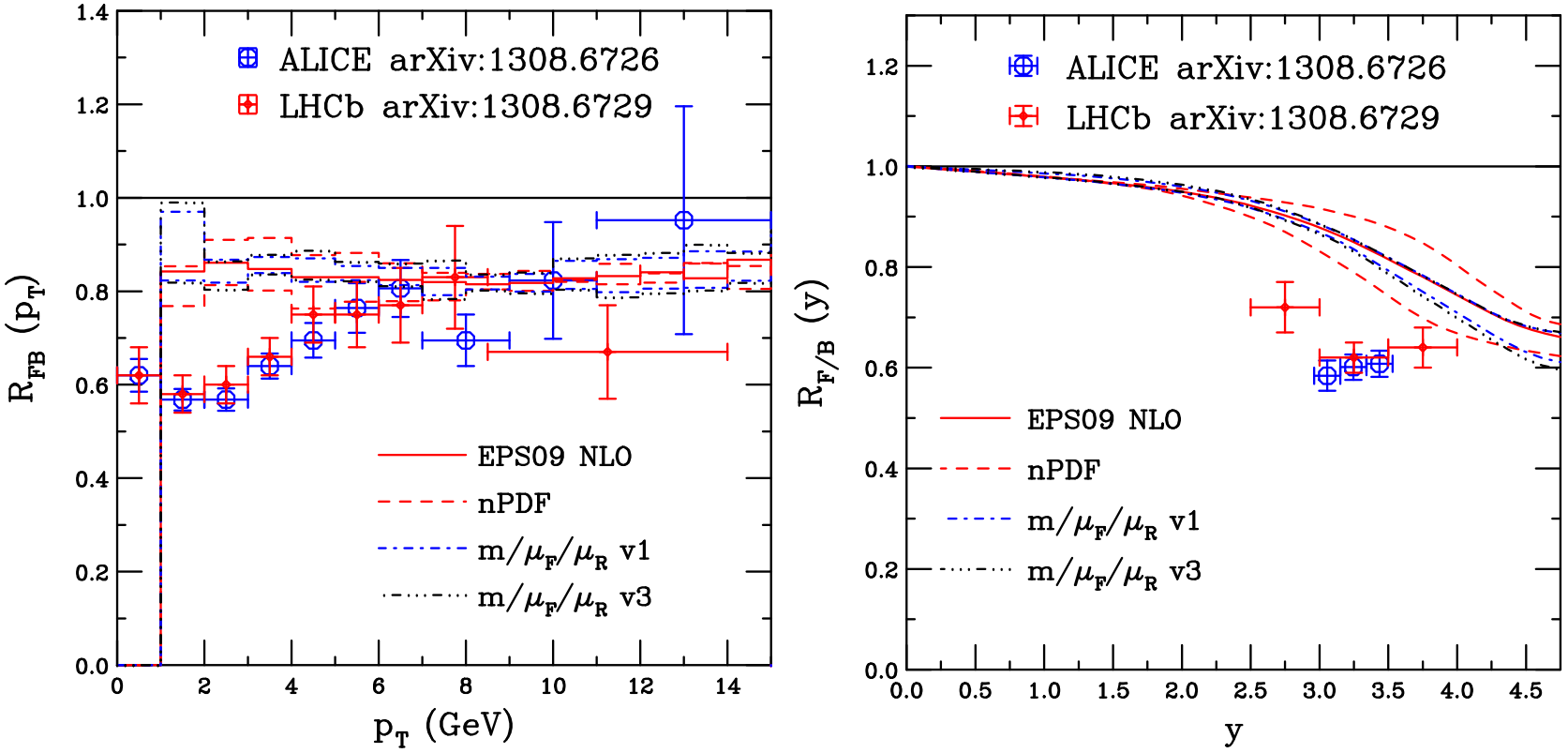

Figure 15: **The mass and scale uncertainties in the ratios $R_{FB}(p_T)$ (left) and $R_{FB}(y)$ (right) are compared to those for EPS09 NLO alone for ALICE at forward (left), backward (middle) and mid- (right) rapidity. The EPS09 uncertainty band is shown in red while the uncertainties calculated with method v1 in blue, v2 in magenta and v3 in black.**

Factorization of R_{AA} into $R_{pA}(+y) \times R_{pA}(-y)$?

The factorization is exact for the CEM at LO because the process is $2 \to 1$ and the scale is fixed ($p_T = 0$) so x_1 and x_2 are known at each y – compare red line with circles on the left

Factorization is not automatic at NLO because process is $2 \to 2\,[(c\overline{c}) + g/q/\overline{q}]$ and the additional parton makes the correspondence between x_1, x_2 and y inexact, even at fixed rapidity – agreement is good, nevertheless

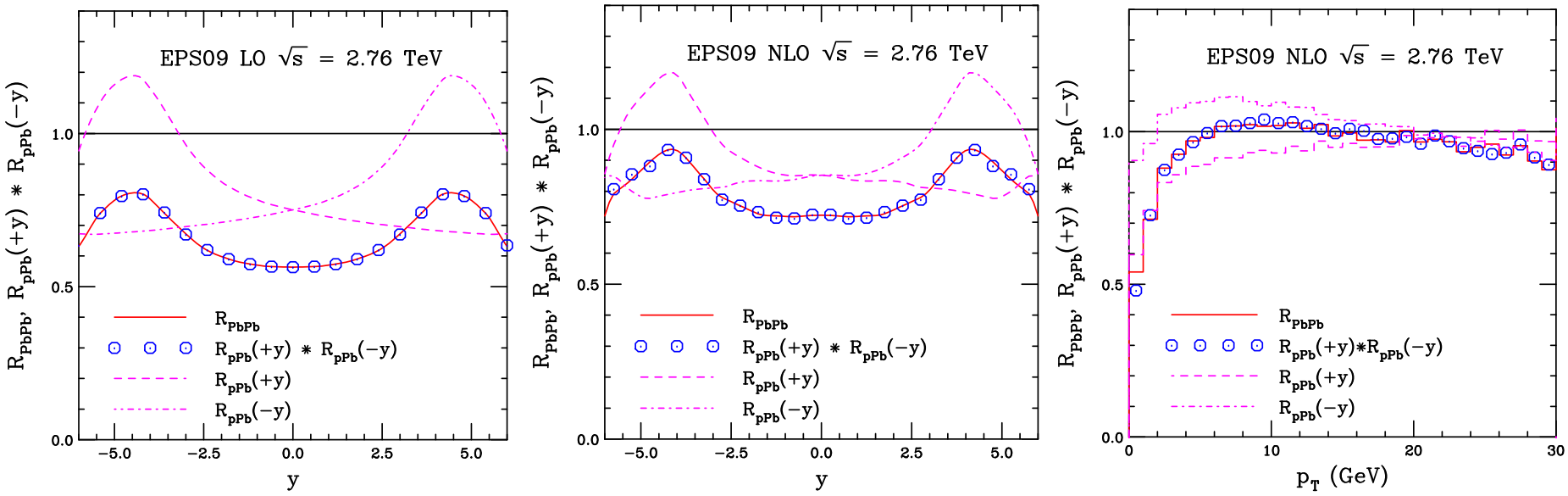

Figure 16: **The R_{AA} (red) ratio is compared to the product $R_{pA}(+y) \times R_{pA}(-y)$ (points) along with the individual pA ratios at forward (dashed) and backward (dot-dashed) rapidity. Results are compared for the rapidity distributions at LO (left) and NLO (middle) as well as for the p_T dependence at NLO (right).**

Summary .

- **Differences in LO and NLO results for EPS09 on J/ψ production illustrates the fact that gluon nPDF is still not very well constrained**
- **LHC p+Pb hadroproduction data could be taken into global analyses in the future but many caveats on medium effects, *e.g.* initial and/or final state energy loss, production mechanism, saturation effects**
- **Υ results available soon**